nature structural & molecular biology

Single-molecule observations of neck linker conformational changes in the kinesin motor protein

Michio Tomishige[1,2], Nico Stuurman[2] & Ronald D Vale[2]

Kinesin-1 is a dimeric motor protein that moves cargo processively along microtubules. Kinesin motility has been proposed to be driven by the coordinated forward extension of the neck linker (a ~12-residue peptide) in one motor domain and the rearward positioning of the neck linker in the partner motor domain. To test this model, we have introduced fluorescent dyes selectively into one subunit of the kinesin dimer and performed 'half-molecule' fluorescence resonance energy transfer to measure conformational changes of the neck linker. We show that when kinesin binds with both heads to the microtubule, the neck linkers in the rear and forward heads extend forward and backward, respectively. During ATP-driven motility, the neck linkers switch between these conformational states. These results support the notion that neck linker movements accompany the 'hand-over-hand' motion of the two motor domains.

Kinesin-1 (conventional kinesin) is a dimeric motor protein that transports cellular cargoes along microtubules within cells[1,2]. Kinesin-1 (hereafter referred to as kinesin) is a highly processive motor that can take ~150 steps in 8-nm increments along a microtubule before dissociating[3–5]. Structural studies using kinesin monomer have suggested how conformational changes, driven by transitions in the ATPase cycle, generate linear motion of kinesin along a microtubule track. Crystal structures have revealed that the compact catalytic core (also termed the 'head') is followed by a short 12-residue peptide (termed the 'neck linker'), which is disordered in some crystal structures[6–8] and ordered and extended along the length of the catalytic core in others[7–11] (**Fig. 1a**, green). A spectroscopic and cryo-EM study performed with truncated kinesin monomers bound to microtubules first revealed that the docked state is favored when the catalytic core contains bound ATP, whereas the undocked state predominates in the nucleotide-free and ADP-bound states[12]. These results prompted a model[13] in which the exchange of ATP for ADP in the leading head of the microtubule-bound kinesin dimer triggers the docking of the neck linker and a ~16-nm displacement of the trailing head upon its release from the microtubule. After a rapid diffusional search, rebinding of the displaced kinesin head to the next available forward tubulin-binding site results in a net 8-nm center-of-mass movement of kinesin. The 16-nm displacement of kinesin heads has recently been measured[14], supporting this 'hand-over-hand' model. Several studies on neck linker conformation also have been interpreted as consistent with this model[15–21]. In addition, an essential role of the neck linker in unidirectional, processive movement has been demonstrated through mutagenesis[22] and cross-linking[23] studies. However, the neck linker conformational state model has been questioned in kinesin dimers, and alternative models for kinesin processivity have been suggested[24,25].

Because of its small size (~12 amino acid residues), developing probes for conformational changes in the neck linker has been challenging. A cryo-EM study has examined neck linker position by inserting a relatively large SH3 domain just distal to the neck linker sequence as an EM marker[16]. This study identified SH3 density between adjacent motor domains bound along a microtubule protofilament in the presence of AMP-PNP (a very slowly hydrolyzable ATP analog), as expected from the neck linker model. However, the individual neck linkers from the forward and rear heads could not be distinguished, and it was not established whether the insertion of the SH3 into the neck linker altered kinesin processivity (although the ATPase activity was shown to be normal). Using a fluorescence-spectroscopy approach, another group has found that two tetramethylrhodamines inserted into both neck linkers of a kinesin dimer show changes in fluorescence (due to rhodamine dimerization), demonstrating that the neck linkers come close together or move apart in a nucleotide-dependent manner[18,19]. A third set of studies[20,21] has taken another approach, measuring neck linker orientation and mobility in a kinesin dimer by fluorescence-polarization microscopy, and again detected nucleotide- and microtubule-dependent changes. Results from these fluorescence approaches[18–21] have supported the neck linker conformational change model for the kinesin dimer and provided further information on how neck linker dynamics are controlled by chemical transitions in the ATPase cycle.

Although previous investigations have provided valuable information on structural states of the kinesin dimer, these studies have either involved averaging a large number of molecules in population

[1]Department of Applied Physics, The University of Tokyo, 7-3-1 Hongo, Bunkyo-ku, Tokyo 113-8656, Japan. [2]Howard Hughes Medical Institute and Department of Cellular and Molecular Pharmacology, University of California, San Francisco, 600 16th Street, San Francisco, California 94158, USA. Correspondence should be addressed to R.D.V. (vale@cmp.ucsf.edu) or M.T. (tomishige@ap.t.u-tokyo.ac.jp).

Received 15 May; accepted 5 September; published online 1 October 2006; doi:10.1038/nsmb1151

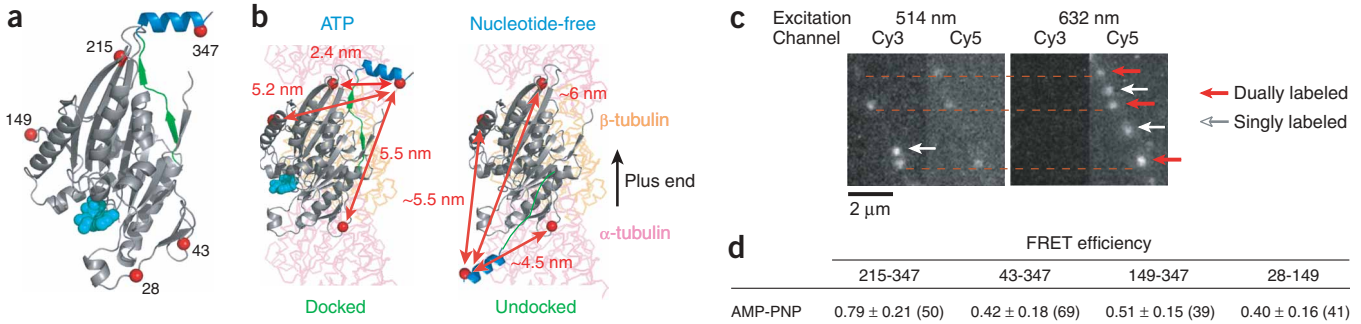

d

	FRET efficiency			
	215-347	43-347	149-347	28-149
AMP-PNP	0.79 ± 0.21 (50)	0.42 ± 0.18 (69)	0.51 ± 0.15 (39)	0.40 ± 0.16 (41)
Apyrase	0.28 ± 0.18 (44)	0.67 ± 0.22 (54)	0.47 ± 0.22 (33)	0.43 ± 0.12 (42)
E236A +ATP	0.81 ± 0.19 (61)	0.34 ± 0.11 (54)		
G234A +ATP	0.37 ± 0.18 (61)	0.81 ± 0.14 (61)		

Figure 1 Single-molecule FRET measurements of monomeric kinesin. (**a**) Positions of cysteines introduced into the cysteine-light kinesin for labeling with thiol-reactive dyes, shown as red spheres on the crystal structure of rat kinesin monomer (PDB entry 2KIN)[9], numbered as in human kinesin. Green, neck linker; blue, neck coiled coil; cyan space-fill, ADP. (**b**) Schematics showing neck linker in docked and undocked states (modeled in the latter case) of a kinesin monomer bound to a microtubule protofilament (1TUB). To determine the neck linker conformation, FRET efficiencies between donor and acceptor fluorophores attached to the neck coiled coil (position 347) and catalytic core (position 43, 149 or 215) were measured. Schematic figures were made with PyMOL (http://pymol.sourceforge.net). (**c**) Images of Cy3 (donor)- and/or Cy5 (acceptor)-labeled kinesin monomers (Cys43-Cys347) bound to an axoneme in the presence of AMP-PNP. Two sets of images were acquired after excitation at 514 and 632 nm (excitation wave lengths of Cy3 and Cy5, respectively), and Cy3 and Cy5 emissions were recorded simultaneously on an intensified CCD camera. Red arrows, single molecules labeled with both Cy3 and Cy5 and showing FRET; white arrows, molecules with only Cy3 or Cy5. (**d**) FRET efficiencies (median ± s.d.) between the indicated dye-position pairs on axoneme-bound monomers in the presence of 1 mM AMP-PNP (ATP-like state) or 5 units ml^{-1} apyrase (nucleotide-free state), or on axoneme-bound E236A or G234A mutant monomers in the presence of 1 mM ATP (see **Supplementary Fig. 2** for histograms). Numbers of molecules analyzed are shown in parentheses. FRET efficiencies for the 215-347 dye pair in the E236A (0.72 ± 0.12; $n = 10$) and G234A (0.45 ± 0.17; $n = 13$) mutants in the presence of 1 mM AMP-PNP were similar to those shown for 1 mM ATP, as expected for these nonhydrolyzing mutants. The means for the 215-347 and 43-347 FRET pairs are significantly different between the AMP-PNP–bound and nucleotide-free states ($P < 0.001$, Kolmogorov-Smirnov test), whereas the 149-347 and 28-149 dye pairs do not show a significant FRET change between these two states ($P > 0.3$). The median values were used to calculate estimated distances between dyes (see Methods). In the presence of AMP-PNP, estimated distances for the 215-347, 43-347 and 149-347 dye pairs are 4.3, 5.6 and 5.3 nm, respectively, which are good approximations of the actual distances between Cα atoms of cysteine residues in the rat kinesin crystal structure (**b**, left). In the presence of apyrase, estimated distances are 6.2, 4.7 and 5.4 nm, respectively (**b**, right).

measurements[16,18–21] or investigated single molecules at saturating ATP concentrations, where conformational transitions within a chemical cycle could not be discerned[20,21]. In addition, previous studies have introduced probes into both neck linkers of the dimer. However, as the two neck linkers are believed to adopt opposing conformations in a processively moving kinesin dimer[13], it would be advantageous to selectively label a single neck linker within the kinesin dimer. In addition, the measurements should be made at a single-molecule level to distinguish these two populations and to detect dynamics in the conformational states of the neck linker. Here, we have introduced donor and acceptor fluorescent dyes selectively into one subunit of the human kinesin-1 dimer and measured fluorescence resonance energy transfer (FRET) at the single-molecule level. We show that the neck linkers in the rear and forward heads extend forward and backward, respectively, when bound to the microtubule in the presence of AMP-PNP, consistent with previous predictions[12,13]. During processive motion at low ATP concentrations, we observed transitions in FRET efficiency, occurring approximately once per 8-nm displacement of the motor. These results support a model in which neck linker movements facilitate hand-over-hand motion of the two motor domains.

RESULTS

Identifying dye-labeling sites for single-molecule FRET

In this study, we used single-molecule FRET (smFRET) to measure conformational states of the neck linker in a microtubule-bound or a processively moving kinesin. We first tested where dyes could be placed in the kinesin dimer without affecting motility (summarized in **Supplementary Fig. 1** online). Various single-cysteine substitutions were introduced into a 'cysteine-light' kinesin homodimer[12,14,23], the protein was labeled with cyanine 3 (Cy3) or tetramethylrhodamine, and the dye-labeled kinesin was tested for processive motility using single-molecule total internal reflection fluorescence microscopy[23]. Of 20 cysteine substitutions tested, 6 did not appreciably affect processive motion. Among these were substitutions just past the end of the neck linker (residue 342) and at the plus end–oriented tip of the catalytic core (residue 215). A dye pair at residues 215 and 342 was therefore selected to monitor the position of the neck linker relative to the catalytic core in dimeric kinesin.

Single-molecule FRET observations of kinesin monomers

To validate our approach for measuring neck linker position, we first determined whether smFRET could detect the nucleotide-dependent conformational changes in the neck linker of a cysteine-light kinesin monomer (K349, residues 1–349 of human ubiquitous kinesin), as previously observed by bulk solution FRET[12]. To monitor the position of the neck linker, Cy3 (donor dye) and Cy5 (acceptor dye) were covalently linked to cysteines introduced just past the end of the neck linker (for monomers, we used residue 347, so as to amplify the nucleotide-dependent FRET efficiency changes) and either at the plus end–oriented tip of the catalytic core (residue 215) or the minus end–oriented base of the core (residue 43) (**Fig. 1a**,**b**). Although the Cy3 and Cy5 maleimide-modified dyes could not be directed to particular cysteines, we could selectively observe individual kinesins that were dually labeled with both dyes (**Fig. 1c**). Cy3 and Cy5 were excited sequentially by laser total internal reflection illumination, and the Cy3

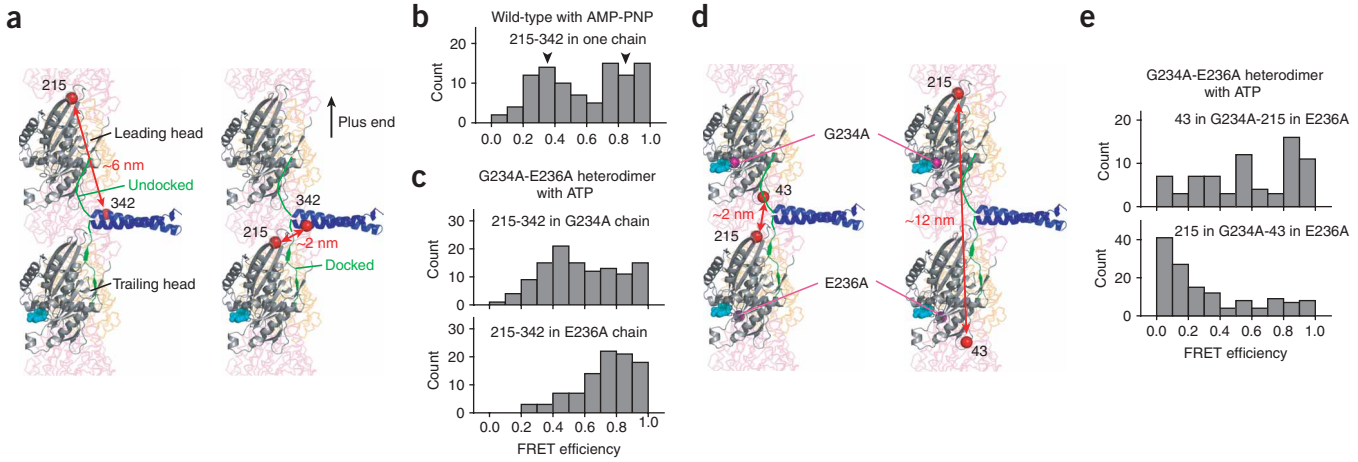

Figure 2 Neck linker positions in microtubule-bound dimeric kinesin in the two-head-bound intermediate state. (**a**) Schematics of the two-head-bound intermediate, based on a model[13] where the neck linker in the leading head points rearward (left; similar to the configuration in **Fig. 1b**, right) and the one in the trailing head is docked onto the catalytic core and points forward (right; also see **Fig. 1b**, left). To examine neck linker conformations, Cys215 and Cys342 (red spheres) were labeled in one chain of the dimer (the other chain is cysteine light and is unreactive to dye labeling). (**b**) Histogram of FRET efficiencies at 215-342 dye pair in one head of microtubule-bound kinesin, in the presence of 1 mM AMP-PNP. Arrowheads mark two clear peaks in FRET efficiency. (**c**) Histograms of FRET efficiencies of axoneme-bound G234A-E236A heterodimeric kinesin in the presence of 1 mM ATP. 215-342 dye pair was introduced into either the G234A subunit (top) or E236A subunit (bottom). Distributions differed significantly depending on which mutant chain contained the dye pair ($P < 0.001$, Kolmogorov-Smirnov test). (**d**) Schematics of G234A-E236A heterodimeric kinesin on the microtubule in the presence of ATP. G234A and E236A residues are shown as magenta spheres. The G234A head (neck linker undocked, extending backward) is predicted to be leading, and the E236A head (neck linker docked, extending forward) to be trailing. To test this, Cys43 and Cys215 were introduced into the two mutant heads as shown. (**e**) Histograms of FRET efficiencies of microtubule-bound G234A-E236A heterodimeric kinesin in the presence of 1 mM ATP. Cys43 and Cys215 were introduced into the two heads as indicated above each chart. The distributions are significantly different ($P < 0.001$).

and Cy5 (or FRET) emissions were recorded simultaneously by spatially separating the two emission wavelengths onto the faceplate of a cooled intensified CCD camera (**Fig. 1c** and Methods). We assured that single molecules were examined, as single photobleaching events of either the Cy3 or Cy5 dye were observed, which resulted in an abrupt loss of the FRET signal (**Supplementary Video 1** online).

We found that the 215-347 dye pair showed greater average smFRET efficiency in the presence of AMP-PNP than under nucleotide-free conditions, whereas the opposite result was obtained with the 43-347 dye pair (**Fig. 1d**; histograms are shown in **Supplementary Fig. 2** online). In fact, nucleotide-dependent differences in FRET efficiencies were greater in this study than those previously obtained by bulk measurements[12], partly owing to differences in the dyes or their positions and possibly also because motors that are singly labeled, unbound to microtubules or inactive can be excluded using single-molecule measurements. As a control, two dyes were placed within the catalytic core itself (28–149) and no nucleotide-dependent change in smFRET efficiency was observed (**Fig. 1d**). The previous study[12] has also identified two ATP-hydrolysis mutations in the switch II region of the nucleotide active site, one of which (E236A) stabilizes the neck linker in the ATP-like, docked conformation whereas the other (G234A) favors the nucleotide-free–like, detached conformation. In the presence of 1 mM ATP, we found that the 215-347 dye pair showed a greater smFRET signal in the E236A mutant than in the G234A mutant, whereas the converse result was obtained with the 43-347 dye pair (**Fig. 1d**). Thus, smFRET generally reveals neck linker positions for microtubule-bound kinesin monomers with various nucleotides and mutations that are similar to the positions reported previously from bulk population FRET measurements and cryo-EM[12].

To model the neck linker structure in the monomer, we estimated the distances between donor and acceptor dyes using the median values of the smFRET efficiencies (see **Fig. 1d** legend and Methods). We acknowledge, however, that these distance estimations are unlikely to be precise because of uncertainties in dye orientation (assumed in our calculations to be random) and location (due to the positioning of the chemical linker, which separates the dye center and the cysteine by ~1.5 nm). Nevertheless, the estimated distances in the presence of AMP-PNP are in good agreement with those observed in the neck linker–docked crystal structure[9] (**Fig. 1b**, left). However, the estimated distances in the nucleotide-free condition differ from what might be expected for a totally disordered neck linker (if the disordered neck linker behaves as an entropic spring, it would be positioned near the base of the neck linker on the core, producing a higher FRET efficiency (~60%) for the 215-347 dye pair). The slight inconsistency might be due to a preferred dye orientation, which would affect the κ^2 value in the Förster distance calculation between the dye pair (see Methods). Alternatively, the neck linker may adopt a backward-extending configuration[26] (**Fig. 1b**, right) in the nucleotide-free state.

Static FRET of microtubule-bound kinesin dimers

We next examined the neck linker positions in a kinesin dimer bound with both heads to a microtubule in the presence of AMP-PNP[27] by selectively introducing FRET reporters into one of the two neck linkers (**Fig. 2a**). To accomplish this, we introduced a cysteine pair (215-342) into a cysteine-light kinesin gene (K490, residues 1–490) bearing a streptavidin tag (Strep tag)[28] and coexpressed it with a cysteine-light K490 with a His_6 tag, then purified the heterodimer by two-step affinity chromatography (see Methods). Heterodimers dually labeled with Cy3 and Cy5 showed processive movement (average velocity at 1 mM ATP was 450 ± 150 nm s^{-1} ($n = 30$), which is similar to that for nonmutant truncated human kinesin fused to green fluorescent protein[29]; **Supplementary Video 2** online). This result indicates that mutation and dye-labeling on these sites in the heterodimer did not

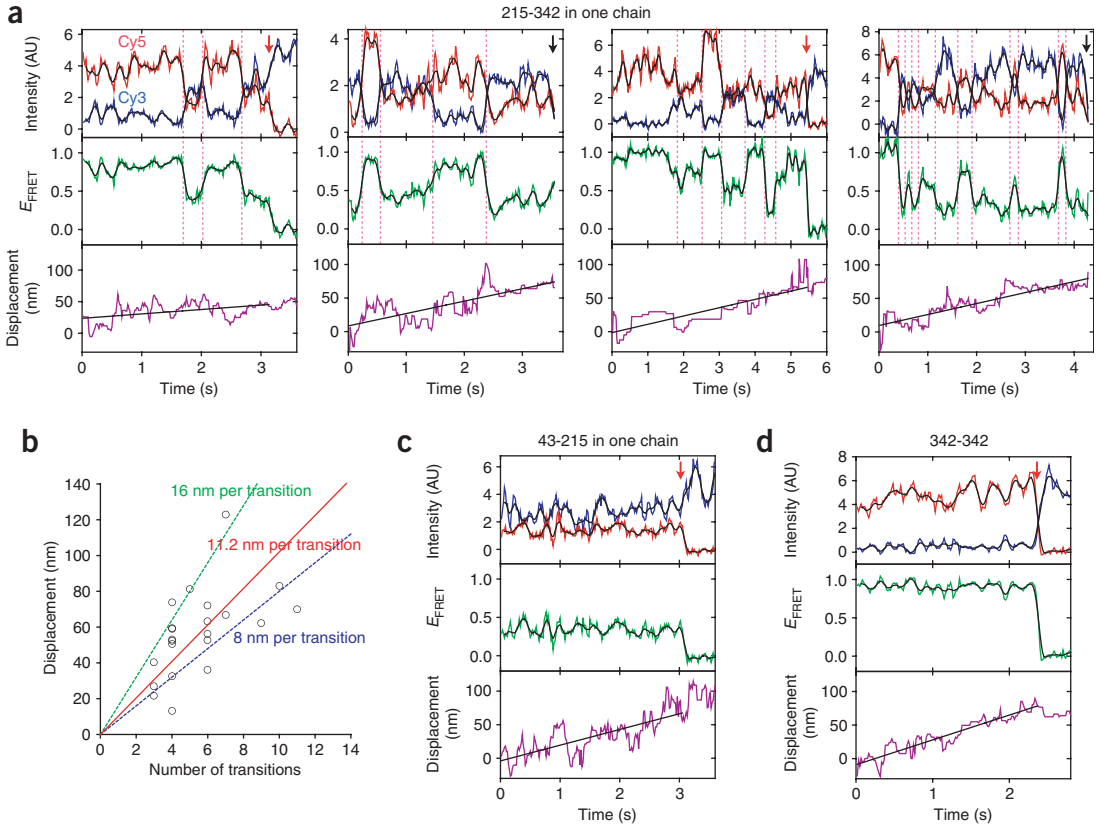

Figure 3 Neck linker conformational changes in kinesin moving along microtubules under low ATP concentrations. (**a**) Four examples of time traces of donor (Cy3, blue) and acceptor (Cy5, red) fluorescence intensities (AU, arbitrary units), calculated FRET efficiency (E_{FRET}, green) and axial displacement of fluorophore centroid (purple), for 215-342 heterodimeric kinesin moving along axonemes in the presence of 0.5 or 1 μM ATP. Images were taken at 60 frames s^{-1} and averaged over four frames. Black lines on fluorescence intensity and E_{FRET} traces show running averages over seven frames. Black lines on displacement traces are linear fits. Vertical magenta dotted lines mark anticorrelated FRET changes (defined as anticorrelated transitions of >0.3 (see Methods)). Red arrows indicate photobleaching of acceptor dye; black arrows indicate photobleaching of donor dye or detachment from the axoneme. (**b**) Relationship between number of transitions and displacement of the motor; each point represents a different single molecule. Transitions were identified on traces, after seven-frame averaging, as large FRET efficiency changes (>0.3) accompanying clear anticorrelations (as marked by dotted vertical lines in **a**). Red line shows linear fit; green and blue lines show predicted relationships. (**c**,**d**) Examples of time traces of parameters in **a**, for 43-215–labeled (**c**) or 342-342–labeled (**d**) heterodimeric kinesin moving along axonemes in the presence of 1 μM ATP, showing little or no conformational change of the catalytic core and no unwinding of the coiled coil on this timescale. See **Supplementary Figures 3** and **5** for additional single-molecule traces.

alter the motor activity (consistent with our previous work on dye-labeled homodimers; **Supplementary Fig. 1**). smFRET efficiencies from this 215-342–labeled, microtubule-bound heterodimer showed a bimodal distribution of low and high FRET efficiencies in the presence of AMP-PNP (**Fig. 2b**). This result is consistent with the neck linker model, in which the 215-342 dye pair in the leading head would have low FRET efficiency (~30% for ~6-nm separation) because its neck linker points backward (**Fig. 2a**, left), whereas the same dye pair in the trailing head would have high FRET efficiency (~100% for ~2-nm separation; **Fig. 2a**, right)[13,26].

In the above heterodimer experiment, the 215-342 dye-labeled head occupied the leading or trailing position with equal probability. To eliminate this heterogeneity and further test the neck linker model, we performed smFRET measurements with a kinesin heterodimer in which one polypeptide chain contained the G234A mutation and the other contained the E236A mutation. In this heterodimer in the presence of ATP, the E236A head is predicted to be in the rear (as its neck linker is locked in for forward-pointing, docked conformation), whereas the G234A head would be leading (with its neck linker detached and pointing backward) (**Fig. 1d**). When the 215-342 dye pair was introduced into the G234A chain of the G234A-E236A heterodimer, the major peak in the FRET efficiency histogram for microtubule-bound heterodimers in the presence of 1 mM ATP was at ~0.4 (**Fig. 2c**, top), although there was a trailing distribution, with higher FRET efficiencies perhaps suggesting some additional conformational states of the motor. In contrast, when the same dye pair was introduced into the E236A chain of the same heterodimer, the major peak in the single-molecule FRET efficiency histogram was at ~0.8 (**Fig. 2c**, bottom). These histograms differ from the bimodal distribution of data from the 215-342 dye pair in the kinesin without the switch II mutations (**Fig. 2b**), indicating that the neck linkers in the leading and trailing heads adopt different configurations.

We also wished to determine the positioning of the mutant heads in the heterodimer by substituting a cysteine in the 215 position of the E236A chain and a cysteine in the 43 position of the G234A chain (**Fig. 2d**, left). This arrangement gave rise to high FRET efficiency for microtubule-bound heterodimers in the presence of ATP (**Fig. 2e**, top), although the distribution was broad owing to noise or perhaps other motor states (for example, one-head-bound states). In contrast, low FRET efficiency was observed with the opposite pairing (Cys215

on the G234A chain and Cys43 on the E236A chain; **Fig. 2d,e**). Thus, the FRET efficiency depended upon dye positioning in the two mutant chains. Together with the results in **Figure 2c**, these data indicate that the E236A chain assumes the position of the trailing head and has its neck linker extending forward, whereas the G234A chain is the leading head and has its neck linker pointing backward. This heterodimer position probably reflects an intermediate in the kinesin motility cycle in which the rear and forward heads are in the ATP-bound and nucleotide-free (or ADP-bound) states, respectively (**Fig. 2a**).

Dynamic FRET of processively moving kinesin dimers

We next wished to determine whether the neck linker changes its conformation when the leading and trailing heads exchange their positions in an active kinesin dimer moving processively along a microtubule. As our acquisition rate was ~60 images s^{-1}, our temporal resolution was insufficient to observe any transient conformations during the kinesin step itself (≤10 ms)[17,18,30], but we could hope to observe the conformation(s) of the kinesin neck linker during the dwell times between steps. To prolong these dwell times, we slowed down kinesin motility by reducing the ATP concentration (~1 μM) so that ATP binding became rate limiting in the cycle. With the neck linker FRET reporter pair (215-342 in one head of the heterodimer), we observed anticorrelated increases and decreases in Cy3 and Cy5 fluorescence, reflecting transitions between high and low FRET efficiencies (**Fig. 3a**; also see **Supplementary Fig. 3** and **Supplementary Videos 3** and **4** online). We simultaneously tracked the centroid of each spot and confirmed that these molecules moved processively along axonemes (**Fig. 3a**, purple), although our method yielded lower spatial resolution than other methods that give lower temporal resolution[14]. We were able to track the centroids of some moving 215-342–labeled heterodimeric kinesin molecules for several seconds before one of the dyes photobleached. In these cases ($n = 22$ molecules), we could estimate the number of anticorrelated transitions in FRET efficiency (120 in total) and the distance traveled (1.25 μm in total) during a particular time period, which equates to a 10.4-nm displacement per FRET transition (**Fig. 3b**). This calculated step size does not agree precisely with the known 8.3-nm kinesin step size[3], but this is not surprising given that transitions with short dwell times could not be detected owing to the limited temporal resolution of our system (see **Supplementary Fig. 4** online). We also measured the dwell times between transitions, which could be fit reasonably well to exponential distributions (**Supplementary Fig. 4**). The mean dwell times in the high and low FRET states were 0.34 and 0.58 s, respectively, which are similar to the expected dwell time of 0.45 s (based on an average motor velocity of 18.5 ± 9.4 nm s^{-1} at 1 μM ATP ($n = 23$)). In summary, these data support the conclusion that anticorrelated changes in Cy3-Cy5 fluorescence are due to conformational changes of the neck linker associated with ATP-driven kinesin stepping.

To confirm that the observed anticorrelated intensity changes represent distance changes between two fluorophores, we introduced a FRET pair at residues 43 and 215 in the catalytic core of one chain of a heterodimer; the distance between these residues is not expected to change substantially during motility[7,8]. With the 43-215 pair, anticorrelated Cy3-Cy5 fluorescence changes (>0.2 FRET efficiency change) were not observed during processive movement in the presence of 1 μM ATP (**Fig. 3c** and **Supplementary Fig. 5** online). We also introduced a FRET pair into the base of the neck coiled coil (Cys342 in both chains) and again found that FRET efficiency was constant during motility (**Fig. 3d** and **Supplementary Fig. 5**). This result also indicates that the base of the coiled coil does not unwind extensively (>3 nm)[23], at least as shown by the temporal inspection available in this study. In addition, use of saturating ATP concentrations (1 mM) with the 215-342 heterodimeric kinesin led to few anticorrelated changes in Cy3-Cy5 fluorescence, as would be expected when the dwell time between steps decreased below our temporal resolution (**Supplementary Fig. 5** and **Supplementary Video 2**). Fluctuations in intensity of a single dye are common, but in these cases, FRET efficiency changes do not exceed 0.2 after seven-frame averaging and are not accompanied by anticorrelated changes in the second dye, as observed clearly for the dynamic neck linker FRET.

DISCUSSION

In this study, we explored conformational states of the neck linker, a proposed mechanical element for motility, in kinesin dimers, using single-molecule FRET. Previous studies[12] have reported a nucleotide- and microtubule-dependent conformational change of the neck linker that represents docking and undocking with the catalytic core in kinesin monomers. Fluorescence reporters[18–21] and markers for EM[16] placed in kinesin dimers have yielded results that are generally consistent with prior monomer studies. Specifically, these kinesin dimer studies have shown that nonhydrolyzable ATP analogs cause the neck linker to adopt a well-ordered forward docked state, whereas the neck linker becomes more flexible in the absence of nucleotide. However, information on the neck linker conformations in the leading and trailing heads has been lacking, as has evidence for alternating structural changes in the neck linkers during hand-over-hand movement. Here, we provide evidence that the neck linkers in the leading and trailing heads adopt different conformations and that individual neck linkers switch between leading and trailing conformations during ATP-driven processive motion (**Fig. 4**). These notions are consistent with a previous model for kinesin processive motility[13] in which ATP-dependent docking of the neck linker in the leading head moves the partner head forward to facilitate its binding to the forward tubulin site.

Dynamic measurements of nucleotide-dependent conformational changes in myosin's 'lever arm' position have been made using FRET[31,32] and at the single-molecule level using fluorescence polarization[33]. However, the small size of kinesin's neck linker (~12 residues) compared with myosin's mechanical element (~130-residue converter domain and lever-arm helix)[34] poses special challenges for measurements of its conformational changes. For example, many cysteine substitutions followed by fluorescent dye labeling result in either partial or complete inactivation of processive motion (**Supplementary Fig. 1**). Even some cysteine labeling (for example, at residues 220 and 333) that preserved the activity of the monomer in prior studies[12] did not yield fully active processive dimers. A likely explanation is that such introduced fluorescent dyes might interfere with head-head interactions or coordination in the kinesin dimer. Thus, successful execution of this work involved testing various positions of dual dye labeling to find ones that allowed normal movement. In addition, measurements of neck linker conformational changes required introducing probes into only one of the two subunits of the kinesin dimers, so as not to generate complex signals from dyes attached to different combinations of the four possible cysteine residues in a homodimer. In this study, selective labeling of one kinesin subunit was achieved by introducing C-terminal protein tags that allowed selective affinity purification of kinesin heterodimers with one cysteine-light subunit and one subunit with two introduced cysteines for dye labeling (or with active site mutations, as was the case with experiments using the G234A-E236A heterodimer).

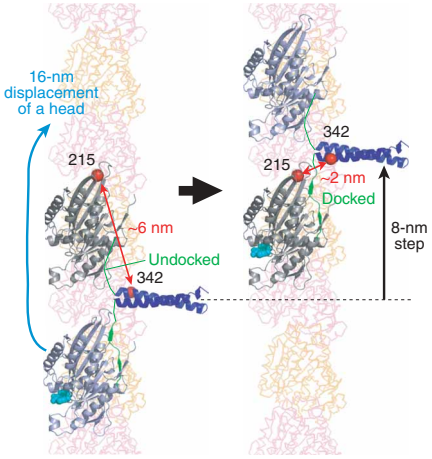

Figure 4 A model consistent with the FRET data shows that the neck linkers switch between backward-extending (undocked) and forward-extending (docked) conformational states during an 8-nm center-of-mass displacement of the kinesin dimer (16-nm movement of trailing head). See text for details as well as an alternative model involving a prolonged one-head-bound intermediate during the dwell time between steps under low ATP concentration.

We detected the neck linker positions in a microtubule-bound kinesin dimer by introducing FRET probes selectively into one of the two neck linkers. FRET efficiencies from microtubule-bound kinesin dimer showed two distinct populations with nearly equal probability, corresponding approximately to the AMP-PNP–bound and nucleotide-free states observed in the monomer. However, the conformations in the leading and trailing heads could not be distinguished by this experiment. To distinguish the two neck linkers in the leading and trailing heads, a G234A-E236A mutant heterodimer proved valuable. Consistent with our expectation from the neck linker model, the G234A head was highly probable in the leading position and the E236A head in the trailing position. Using this heterodimer, we also provide the first evidence for the neck linker conformational states in this two-head-bound state: the neck linker is pointing forward in the trailing head (ATP-like state; E236A) and pointing backward in the leading head (nucleotide-free state; G234A). The forward-extending neck linker in the trailing head is likely to reflect the state observed in crystal structures where the neck linker is docked on the catalytic core[7–11]. However, the precise conformation of the backward-pointing neck linker remains uncertain. One possibility is that this neck linker is highly mobile, constrained to point rearward by a connection to the rear head through the coiled-coil domain; measurements that assess neck linker flexibility support this view[12,15,16,21]. A second possibility is that the backward-pointing neck linker is docked to a specific site on the catalytic core[26], as has been observed for a related kinesin (kinesin-5 or Eg5)[35]. Such a backward-docked conformation might facilitate ADP release when the detached head rebinds to a forward tubulin-binding site[20,36]. Our measurements of FRET efficiency with nucleotide-free kinesin monomers can also be interpreted in favor of a backward-docked state, although caveats exist (such as effects of dye labeling on protein conformation and uncertainties in dye orientation for FRET distance calculations). The existence of a nucleotide-free docked state therefore merits further investigation using different probes.

In this study, we also observed FRET efficiency changes of a dye pair in a single neck linker within a kinesin dimer during slow processive movement under low ATP concentrations. On average, these transitions took place approximately once per 8-nm step, although we lacked sufficient spatiotemporal resolution to show that FRET transitions occurred simultaneously with an 8-nm step. Nonetheless, our results provide the first direct evidence for alternating neck linker conformational changes during processive movement.

The dynamic FRET measurements also provide some insight into the 'waiting' state of kinesin at low ATP concentrations, which has been subject to various interpretations (reviewed in ref. 25). One model proposes that kinesin waits for the next ATP as a one-head-bound intermediate, in which one head is bound tightly to the microtubule (nucleotide-free 'waiting' head) whereas the ADP-bound partner head is detached and potentially poised in a position for the next forward step[4,30]. However, recent kinetic and fluorescence-polarization data suggest that the ADP-bound head may also be tethered to the microtubule but incapable of rapidly releasing ADP, perhaps because of the forward neck linker position in this two-head-bound intermediate[20,37]. Our results show that a single neck linker in a kinesin molecule alternates between two FRET states during processive motion, which is most consistent with a two-head-bound intermediate state. If the kinesin moved in an 'inchworm' manner[38] or with a consistent one-head-bound intermediate state (with two mobile neck linkers in the nucleotide-free and ADP-bound head), then less obvious FRET transitions would be expected. However, alternate FRET transitions might be observed with a one-head-bound intermediate if the neck linker on the waiting, nucleotide-free head adopted a backward-pointing structure (FRET efficiency changes would then represent transitions between an ordered, nucleotide-free and a disordered, ADP-bound state). In addition, it is possible that the two models may not be absolute, as two-head-bound and one-head-bound conformations may both occur for kinesin molecules moving at low ATP concentrations. Answering the question of whether kinesin waits with one head or two heads bound (or both) will require measuring the spacing between the heads during motility. Single-molecule FRET measurements of head-head positioning with improved temporal resolution will provide a powerful tool for such investigations.

In conclusion, single-molecule FRET reporters provide evidence for distinct conformations of the neck linkers in a kinesin dimer. In a static two-head-bound kinesin dimer, we show that the neck linkers extend forward and backward in the trailing and leading heads, respectively, and that these conformational states alternate during ATP-driven processive motility. This data, in conjunction with previous FIONA measurements[14] and other studies showing alternation in kinesin stepping behavior[39–41], support models in which the neck linker movements facilitate the hand-over-hand stepping of the kinesin heads during processive motility (**Fig. 4**).

METHODS

DNA cloning. Cysteines (K28C, S43C, S149C, E215C, K342C, E347C) and/or mutations in the switch II region (E236A, G234A) were introduced into a cysteine-light human ubiquitous kinesin 349-residue[12] monomer or a dimer of 490-residue subunits, each containing a C-terminal His_6 tag. For heterodimers, a coexpression vector was constructed that carries two 490-residue kinesin sequences in tandem: the first kinesin sequence contains a C-terminal streptavidin tag (Strep tag; 9 residues, AWRHPQFGG)[28] and the second is followed by a His_6 tag. Each kinesin gene has its own ribosome-binding site, and the two genes are flanked by a T7 promoter and a T7 terminator. All constructs were verified by DNA sequencing.

Protein purification. Monomeric kinesins were expressed and purified as described[23]. Heterodimeric kinesins were expressed, then purified from lysates by nickel–nitrilotriacetic acid chromatography as described[23]. Heterodimers

were further purified by Strep-Tactin (streptavidin mutant) affinity purification[28]. Eluate from nickel–nitrilotriacetic acid resin was loaded on a Strep-Tactin Sepharose (IBA GmbH) column, and then washed with ST buffer (50 mM phosphate buffer (pH 7.0), 250 mM NaCl, 2 mM $MgCl_2$, 10 mM 2-mercaptoethanol, 100 μM ATP). Heterodimers were eluted with ST buffer containing 2.5 mM D-desthiobiotin. Purified monomeric and heterodimeric kinesins were dialyzed against 25 mM PIPES (pH 7.0), 100 mM NaCl, 1 mM EGTA, 2 mM $MgCl_2$ and 50 μM ATP for 4 h at 4 °C. Protein concentrations were determined by Bradford assays using BSA as a standard. Typical yields of heterodimer proteins were 0.2–0.5 mg from 1 l of bacterial culture. Dialyzed kinesin was reacted with Cy3-maleimide and Cy5-maleimide (Amersham Biosciences) at a motor head/Cy3 dye/Cy5 dye molar ratio of 1:10:10, for 4 h at 4 °C. Unreacted dyes were quenched with 1 mM DTT and then removed through microtubule affinity purification as described[23], except that 100 μM ATP was used for releasing motors from microtubules.

Single-molecule fluorescence microscopy. Single-molecule FRET microscopy was based on a custom-built total internal reflection fluorescence microscope as described[23,29]. Dye-labeled heterodimeric kinesins were attached onto the axonemes (purified from sea urchin sperm flagella) in the presence of 1 mM AMP-PNP or 5 units ml^{-1} apyrase, or moved along axonemes in the presence of ATP and an ATP-regenerating system as described[29]. The dye-labeled monomers were bound to axonemes at a density where single fluorescent molecules could be clearly distinguished. Cy3 and Cy5 dyes were illuminated with an argon laser (514 nm) and a helium-neon laser (632 nm), respectively (10–20 mW laser power). The fluorescence images from Cy3 and Cy5 (or FRET) were separated using Dual-View (Optical Insights) and then projected side by side on a cooled, intensified CCD camera (XR/MEGA10-Z, Stanford Photonics) or an intensified CCD camera (XR/MEGA10, Stanford Photonics) with acquisition rates of 60 frames s^{-1}. For the static FRET measurements, both Cy3 and Cy5 fluorophores were directly illuminated by sequential excitation with the argon and helium-neon lasers. Both lasers were used to identify molecules that showed little or no FRET (that is, molecules labeled with both Cy3 and Cy5, but that did not emit in the Cy5 channel after excitation of Cy3). For the dynamic FRET measurements, it was not possible to use alternating laser excitation and retain sufficient temporal information on the FRET signal, and instead images were taken by excitation with the argon laser.

Data analysis. Images for static FRET efficiencies were analyzed using Image J (http://rsb.info.nih.gov/ij/) with custom-designed plug-in software. Images for donor or acceptor excitations were averaged over ~120 frames. This set of images was used to identify Cy3-Cy5 dually labeled motors and their Cy3 and Cy5 fluorescence intensities. Axonemes that were sparsely coated with fluorescence spots (less than 1 spot per 2-μm microtubule (~35 pixels)) were used for data analysis to reduce the chance that two distinct Cy3 and Cy5 spots happened to colocalize on the axonemes within one pixel (57 nm). FRET efficiencies were calculated as $E = 1/(1 + I_D/(I_A - \chi I_D)\gamma)$, where I_D and I_A are background-subtracted intensities from the donor and acceptor channels, respectively, χ is the cross-talk of donor intensity into acceptor channel and γ is a parameter to correct for different detection efficiencies of the two channels and the quantum yields of donor and acceptor dyes. χ was determined experimentally by observing donor only–labeled motors, and γ was determined by observing the donor and acceptor intensity changes after photobleaching of the acceptor dye in motors showing ~100% FRET (342-342 mutants; **Supplementary Video 1**). Cy5 intensities corrected as $(I_A - \chi I_D)\gamma$ are shown in figures for time traces. The distances r between donor and acceptor dyes were estimated using the relationship $E = (1 + (r/R_0)^6)^{-1}$, where $R_0 = 5.3$ nm was used as the Förster radius (assuming a constant orientation factor κ^2 of 2/3)[42]. Images for dynamic FRET measurements were averaged over four frames and then analyzed using custom-designed MATLAB software (The MathWorks). Background-subtracted fluorescence intensities from the donor and acceptor channels were determined for each frame and the corrected FRET efficiencies were determined as described above. Centroids of the fluorescence spots were tracked using a cross-correlation algorithm[43]. Fluorescence spots that did not show clear unidirectional movement (motor was inactive or its displacement was small compared to the noise) were not subjected to further data analysis. Analyses were also only done on spots that showed decent signal-to-noise ratio in fluorescence intensities, minimal blinking, slow movement (<40 nm s^{-1}) and long duration before photobleaching or detachment from the microtubule. To identify anticorrelated transitions, we first applied a seven-frame running-average filter to the FRET efficiency traces to reduce the noise and then identified transitions that accompany large FRET efficiency changes (>0.3).

Note: Supplementary information is available on the Nature Structural & Molecular Biology website.

ACKNOWLEDGMENTS

We thank K. Thorn for development of the initial version of the microscope system and for discussions, and U. Wiedemann for support in cloning and protein purification. M.T. is supported by grants from the Mitsubishi Foundation, Asahi Glass Foundation, Sumitomo Foundation and Inamori Foundation and by Grants-in-Aid for Scientific Research on Priority Areas. R.D.V. is supported by grants from the Howard Hughes Medical Institute and the US National Institutes of Health.

AUTHOR CONTRIBUTIONS

M.T. and R.D.V. conceived and designed the experiments. M.T. performed the experiments and data analysis. N.S. contributed to microscope construction and programming. R.D.V. and M.T. discussed the results and wrote the manuscript.

COMPETING INTERESTS STATEMENT

The authors declare that they have no competing financial interests.

Published online at http://www.nature.com/nsmb/
Reprints and permissions information is available online at http://npg.nature.com/reprintsandpermissions/

1. Vale, R.D. The molecular motor toolbox for intracellular transport. *Cell* **112**, 467–480 (2003).
2. Hirokawa, N. & Takemura, R. Molecular motors and mechanisms of directional transport in neurons. *Nat. Rev. Neurosci.* **6**, 201–214 (2005).
3. Svoboda, K., Schmidt, C.F., Schnapp, B.J. & Block, S.M. Direct observation of kinesin stepping by optical trapping interferometry. *Nature* **365**, 721–727 (1993).
4. Hackney, D.D. Evidence for alternating head catalysis by kinesin during microtubule-stimulated ATP hydrolysis. *Proc. Natl. Acad. Sci. USA* **91**, 6865–6869 (1994).
5. Vale, R.D. *et al.* Direct observation of single kinesin molecules moving along microtubules. *Nature* **380**, 451–453 (1996).
6. Kull, F.J., Sablin, E.P., Lau, R., Fletterick, R.J. & Vale, R.D. Crystal structure of the kinesin motor domain reveals a structural similarity to myosin. *Nature* **380**, 550–555 (1996).
7. Kikkawa, M. *et al.* Switch-based mechanism of kinesin motors. *Nature* **411**, 439–445 (2001).
8. Nitta, R., Kikkawa, M., Okada, Y. & Hirokawa, N. KIF1A alternatively use two loops to bind microtubules. *Science* **305**, 678–683 (2004).
9. Sack, S. *et al.* X-ray structure of motor and neck domains from rat brain kinesin. *Biochemistry* **36**, 16155–16165 (1997).
10. Kozielski, F. *et al.* The crystal structure of dimeric kinesin and implications for microtubule-dependent motility. *Cell* **91**, 985–994 (1997).
11. Sindelar, C.V. *et al.* Two conformations in the human kinesin power stroke defined by X-ray crystallography and EPR spectroscopy. *Nat. Struct. Biol.* **9**, 844–848 (2002).
12. Rice, S. *et al.* A structural change in the kinesin motor protein that drives motility. *Nature* **402**, 778–784 (1999).
13. Vale, R.D. & Milligan, R.A. The way things move: looking under the hood of molecular motor proteins. *Science* **288**, 88–95 (2000).
14. Yildiz, A., Tomishige, M., Vale, R.D. & Selvin, P.R. Kinesin walks hand-over-hand. *Science* **303**, 676–678 (2004).
15. Rice, S. *et al.* Thermodynamic properties of the kinesin neck-region docking to the catalytic core. *Biophys. J.* **84**, 1844–1854 (2003).
16. Skiniotis, G. *et al.* Nucleotide-induced conformations in the neck region of dimeric kinesin. *EMBO J.* **22**, 1518–1528 (2003).
17. Rosenfeld, S.S., Jefferson, G.M. & King, P.H. ATP reorients the neck linker of kinesin in two sequential steps. *J. Biol. Chem.* **276**, 40167–40174 (2001).
18. Rosenfeld, S.S., Xing, J., Jefferson, G.M., Cheung, H.C. & King, P.H. Measuring kinesin's first step. *J. Biol. Chem.* **277**, 36731–36739 (2002).
19. Rosenfeld, S.S., Fordyce, P.M., Jefferson, G.M., King, P.H. & Block, S.M. Stepping and stretching: how kinesin uses internal strain to walk processively. *J. Biol. Chem.* **278**, 18550–18556 (2003).
20. Asenjo, A.B., Krohn, N. & Sosa, H. Configuration of the two kinesin motor domains during ATP hydrolysis. *Nat. Struct. Biol.* **10**, 836–842 (2003).
21. Asenjo, A.B., Weinberg, Y. & Sosa, H. Nucleotide binding and hydrolysis induces a disorder-order transition in the kinesin neck-linker region. *Nat. Struct. Mol. Biol.* **13**, 648–654 (2006).
22. Case, R.B., Rice, S., Hart, C.L., Ly, B. & Vale, R.D. Role of the kinesin neck linker and catalytic core in microtubule-based motility. *Curr. Biol.* **10**, 157–160 (2000).

23. Tomishige, M. & Vale, R.D. Controlling kinesin by reversible disulfide cross-linking: identifying the motility-producing conformational change. *J. Cell Biol.* **151**, 1081–1092 (2000).
24. Schief, W.R. & Howard, J. Conformational changes during kinesin motility. *Curr. Opin. Cell Biol.* **13**, 19–28 (2001).
25. Carter, N.J. & Cross, R.A. Kinesin's moonwalk. *Curr. Opin. Cell Biol.* **18**, 61–67 (2006).
26. Sablin, E.P. & Fletterick, R.J. Coordination between motor domains in processive kinesins. *J. Biol. Chem.* **279**, 15707–15710 (2004).
27. Kawaguchi, K. & Ishiwata, S. Nucleotide-dependent single- to double-headed binding of kinesin. *Science* **291**, 667–669 (2001).
28. Skerra, A. & Schmidt, T.G. Applications of a peptide ligand for streptavidin: the Strep-tag. *Biomol. Eng.* **16**, 79–86 (1999).
29. Tomishige, M., Klopfenstein, D.R. & Vale, R.D. Conversion of Unc104/KIF1A kinesin into a processive motor after dimerization. *Science* **297**, 2263–2267 (2002).
30. Carter, N.J. & Cross, R.A. Mechanics of the kinesin step. *Nature* **435**, 308–312 (2005).
31. Suzuki, Y., Yasunaga, T., Ohkura, R., Wakabayashi, T. & Sutoh, K. Swing of the lever arm of a myosin motor at the isomerization and phosphate-release steps. *Nature* **396**, 380–383 (1998).
32. Shih, W.M., Gryczynski, Z., Lakowicz, J.R. & Spudich, J.A. A FRET-based sensor reveals large ATP hydrolysis-induced conformational changes and three distinct states of the molecular motor myosin. *Cell* **102**, 683–694 (2000).
33. Forkey, J.N., Quinlan, M.E., Shaw, M.A., Corrie, J.E. & Goldman, Y.E. Three-dimensional structural dynamics of myosin V by single-molecule fluorescence polarization. *Nature* **422**, 399–404 (2003).
34. Houdusse, A., Kalabokis, V.N., Himmel, D., Szent-Györgyi, A.G. & Cohen, C. Atomic structure of scallop myosin subfragment S1 complexed with MgADP: a novel conformation of the myosin head. *Cell* **97**, 459–470 (1999).
35. Turner, J. *et al.* Crystal structure of the mitotic spindle kinesin Eg5 reveals a novel conformation of the neck-linker. *J. Biol. Chem.* **276**, 25496–25502 (2001).
36. Kinosita, K., Jr. *et al.* How two-foot molecular motors may walk. *Adv. Exp. Med. Biol.* **565**, 205–219 (2005).
37. Hackney, D.D. The tethered motor domain of a kinesin-microtubule complex catalyzes reversible synthesis of bound ATP. *Proc. Natl. Acad. Sci. USA* **102**, 18338–18343 (2005).
38. Hua, W., Chung, J. & Gelles, J. Distinguishing inchworm and hand-over-hand processive kinesin movement by neck rotation measurements. *Science* **295**, 844–848 (2002).
39. Asbury, C.L., Fehr, A.N. & Block, S.M. Kinesin moves by an asymmetric hand-over-hand mechanism. *Science* **302**, 2130–2134 (2003).
40. Kaseda, K., Higuchi, H. & Hirose, K. Alternate fast and slow stepping of a heterodimeric kinesin molecule. *Nat. Cell Biol.* **5**, 1079–1082 (2003).
41. Higuchi, H., Bronner, C.E., Park, H.-W. & Endow, S.A. Rapid double 8-nm steps by a kinesin mutant. *EMBO J.* **23**, 2993–2999 (2004).
42. Ishii, Y., Yoshida, T., Funatsu, T., Wazawa, T. & Yanagida, T. Fluorescence resonance energy transfer between single fluorophores attached to a coiled-coil protein in aqueous solution. *Chem. Phys.* **247**, 163–173 (1999).
43. Gelles, J., Schnapp, B.J. & Sheetz, M.P. Tracking kinesin-driven movements with nanometre-scale precision. *Nature* **331**, 450–453 (1988).

Erratum: Single-molecule observations of neck linker conformational changes in the kinesin motor protein

Michio Tomishige, Nico Stuurman & Ronald D Vale

Nat. Struct. Mol. Biol. **13, 887–894 (2006); published online 1 October 2006; corrected after print 7 November 2006**

In the supplementary information initially published online to accompany this article, the Supplementary Video legends were inadvertently excluded. The error has been corrected online.